Kirchgessner, T. G., Chaut, J. C., Heinzmann, C., Etienne, J., Guilhot, S., Svenson, K., Ameis, D., Pilon, D., D'Auriol, L., Audalibi, A., Schotz, M. C., Galibert, F., & Lusis, A. J. (1989) *Proc. Natl. Acad. Sci. U.S.A. 86*, 9647-9651.
Komaromy, M. C., & Schotz, M. C. (1987) *Proc. Natl. Acad. Sci. U.S.A. 84*, 1526-1530.
Laboda, H. M., Glick, J. M., & Phillips, M. C. (1986) *Biochim. Biophys. Acta 876*, 233-242.
Lee, K. K., & Ellis, A. E. (1990) *J. Bacteriol. 172*, 5382-5393.
Maraganore, J. M., & Heinrikson, R. L. (1986) *Trends Biochem. Sci. (Pers. Ed.) 11*, 497-498.
Neville, D. M. (1971) *J. Biol. Chem. 246*, 6328-6334.
Pattus, F., Slotboom, A. V., & de Haas, G. H. (1979) *Biochemistry 18*, 2691-2697.
Persson, B., Bengtsson-Olivecrona, G., Enerback, S., Olivecrona, T., & Jornvall, H. (1989) *Eur. J. Biochem. 179*, 39-45.
Phillips, M. C., & Chapman, D. (1968) *Biochim. Biophys. Acta 163*, 301-313.
Rietsch, J., Pattus, F., Desnuelle, P., & Verger, R. (1977) *J. Biol. Chem. 252*, 3128-3133.
Thornton, J., Howard, S. P., & Buckley, J. T. (1988) *Biochim. Biophys. Acta 959*, 153-159.
Vainio, P., Virtanen, J. A., Kinnunen, P. K. J., Voyta, J. C., Smith, L. C., Gotto, A. M., Jr., Sparrow, J. T., Pattus, F., & Verger, R. (1983) *Biochemistry 22*, 2270-2275.
Verger, R., & de Haas, G. H. (1973) *Chem. Phys. Lipids 10*, 127-136.
Verger, R., & Pattus, F. (1982) *Chem. Phys. Lipids 30*, 189-227.
Verger, R., Mieras, M. C. E., & de Haas, G. H. (1973) *J. Biol. Chem. 248*, 4023-4034.
Verger, R., Rietsch, J., van Dam-Mieras, M. C. E., & de Haas, G. H. (1976) *J. Biol. Chem. 251*, 3128-3133.
Winkler, F. K., D'Arcy, A., & Hunziker, W. (1990) *Nature 343*, 771-774.
Wion, K. L., Kirchgessner, T. G., Lusis, A. J., Schotz, M. C., & Lawn, R. (1987) *Science 235*, 1638-1641.

Raman Spectroscopic Characterization of Tryptophan Side Chains in Lysozyme Bound to Inhibitors: Role of the Hydrophobic Box in the Enzymatic Function†

Takashi Miura, Hideo Takeuchi, and Issei Harada*
Pharmaceutical Institute, Tohoku University, Aobayama, Sendai 980, Japan
Received December 12, 1990; Revised Manuscript Received March 28, 1991

ABSTRACT: The state of H-bonding and the hydrophobic interaction of six tryptophan side chains in lysozyme bound to substrate-analogous inhibitors were investigated by combining H → D exchange labeling and Raman difference spectroscopy. The frequency of the W17 band due to Trp-63 shifts downward upon inhibitor binding, indicating a specific and strong H-bond formation between the N_1 site of the side chain and the inhibitor molecule. On the other hand, the H-bonding state of Trp-62 in the complex is as weak as that in inhibitor-free lysozyme, suggesting no contribution of this residue to the inhibitor binding. Intensity increases of W17 and W18 bands observed upon inhibitor binding are, respectively, ascribed to an increase at Trp-28 and a decrease at Trp-111 in hydrophobic interactions with the environment. The environmental changes are explained consistently by a movement of the Met-105 side chain sandwiched by two indole rings of Trp-28 and 111 in the direction from Trp-111 to Trp-28. The sandwich structure in a core domain, hydrophobic box, and its rearrangement are considered to play an important role in the enzymatic function of lysozyme.

Lysozyme catalyzes the hydrolysis of β-1,4-glycosidic linkages of cell-wall mucopolysaccharides (Jeanloz et al., 1963) and chitin (Berger & Weiser, 1957), a polymer of *N*-acetyl-D-glucosamine. The amino acid composition of hen egg white lysozyme is characterized by high contents of tryptophan (6 Trp at sequence positions 28, 62, 63, 108, 111, and 123 among 129 residues) as well as cystine (4 Cys–Cys) and basic residues (11 Arg + 6 Lys). According to an X-ray diffraction study on a tetragonal crystal of the lysozyme–inhibitor complex (Blake et al. 1967), the active site is composed of six subsites, named A through F, which accommodate six consecutive saccharide units. In subsite C, Trp-62 and -63 are exposed at the edge of active site cleft, and Trp-108 is partially buried underneath the active site. Trp-62 and -63 interact specifically with the inhibitor through hydrogen bonds (H-bonds)[1] from their indole N_1H groups to the oxygen atoms of a saccharide unit that binds to site C. In a recent X-ray study on an orthorhombic form crystallized at 38 °C, however, the H-bond between Trp-62 and the incorporated inhibitor was not found (Bernard et al., 1990). In aqueous solution, on the other hand, the lysozyme–inhibitor interaction has been examined by NMR. The N_1H NMR signals of Trp-63 and -108 shift upon inhibitor binding, but that of Trp-62 remains practically un-

† This work was supported by a Grant-in-Aid for Encouragement of Young Scientists (No. 02953072) and a Grant-in-Aid for General Scientific Research (No. 62430004) from the Ministry of Education, Science, and Culture.
* To whom correspondence should be addressed.

[1] Abbreviations: GlcNAc, an equilibrium mixture of the α- and β-form of *N*-acetyl-D-glucosamine; $(GlcNAc)_3$, *N*,*N*′,*N*″-triacetylchitotriose; Ac-L-TrpME, *N*-acetyl-L-tryptophan methyl ester; Ac-DL-TrpMA, *N*-acetyl-DL-tryptophan methylamide; L-Trp·HCl, L-tryptophan hydrochloride; H-bond, hydrogen bond; NMR, nuclear magnetic resonance.

0006-2960/91/0430-6074$02.50/0

shifted (Blake et al., 1981), suggesting the absence of a specific interaction between Trp-62 and the bound inhibitor in solution, in accord with the structure of the orthorhombic crystal.

Shifts of ^1H and ^{13}C NMR signals upon inhibitor binding have been observed also for other side chains, especially in a hydrophobic domain called a "hydrophobic box" (Perkins & Dwek, 1980; Blake et al., 1981; Bernard et al., 1990). The hydrophobic box was found in a 2-Å resolution electron density map of a core region of lysozyme as a clearly identifiable set of side chains, i.e., Trp-28, -108, and -111 together with Tyr-23 and Met-105 (Blake et al., 1965). Although these side chains are adjacent to the active site cleft, they do not directly interact with the inhibitor molecule with the exception of Trp-108 (Blake et al., 1967). Accordingly, the observed NMR shifts have been ascribed to conformational changes in the hydrophobic box (Blake et al., 1981). The shifts of NMR signals may, however, have resulted from complex effects of H-bonding and magnetic anisotropy of adjacent groups and can not be immediately correlated with one of such factors.

The purpose of the present work is to obtain information on the strength of H-bonding and the environments of tryptophan side chains in aqueous lysozyme bound to an inhibitor through Raman spectroscopy. Recently, we proposed a combined method of hydrogen–deuterium exchange labeling and Raman difference spectroscopy to investigate the states of individual tryptophan side chains in proteins and succeeded in characterizing the six tryptophans in aqueous lysozyme solution (Miura et al., 1988). This method was applied to lysozyme–inhibitor complexes in the present work. The strength of H-bonding or hydrophobic interaction is reflected in the frequencies and/or intensities of Raman bands. The frequency of a band around 877 cm^{-1} (named W17; Harada & Takeuchi, 1986) varies with the strength of H-bonding at the N_1H site of tryptophan (Miura et al., 1988). Thus the strength of an H-bond between a tryptophan side chain and an incorporated inhibitor can be evaluated from the W17 frequency. As a marker of hydrophobicity around tryptophyl indole, the intensity of the 1360-cm^{-1} band was employed in the previous study (Miura et al., 1988). However, this band could not be used in this study because of overlap with an inhibitor band. Instead, other bands providing similar information have been found and used. Here, we report the strength of H-bonding of six tryptophan side chains in lysozyme–inhibitor complexes and structural changes in the hydrophobic box upon inhibitor binding.

Experimental Procedures

Lysozyme from hen egg white (EC 3.2.1.17, three-times crystallized, dialyzed, and lyophilized) and α-*N*-acetyl-D-glucosamine (α-GlcNAc) were obtained from Sigma Chemical. Lysozyme was further purified by crystallization, dialysis, and lyophilization. *N,N',N''*-triacetylchitotriose [$(GlcNAc)_3$] was prepared from chitin by hydrolysis (Rupley, 1964). Skatole (3-methylindole) was obtained from Nacalai Tesque. The protein concentration was 10 mM throughout the experiments. The inhibitor concentrations were 200 mM for GlcNAc [about 90% binding according to the association constants listed by Imoto et al. (1972)] and 20 mM for $(GlcNAc)_3$ (100% binding), respectively. The pH (pD) adjustments of aqueous protein were made with aqueous HCl (DCl) and NaOH (NaOD) and determined on a Hitachi-Horiba M-7II pH meter.

Raman spectra were obtained with a multichannel detection system described previously (Harada et al., 1986). Typical experimental conditions were as follows: excitation wavelength, 488 nm; laser power, 100 mW; spectral slit width, 5 cm^{-1}; data accumulation, 600 s; temperature, 23 ± 1 °C. Raman spectra of proteins deuteriated at low temperatures (below 23 °C) were measured at those temperatures by use of a thermostated cell. The wave number axis of the Raman spectra was calibrated for indene, and peak positions were reproducible to within ±1 cm^{-1}. The reproducibility of relative intensities was better than 2%. ^1H NMR spectra were recorded at 500 MHz on a JNM-GX500 spectrometer with an external reference of 1% tetramethylsilane in chloroform-*d*.

Deuterium Exchange Labeling. Various factors such as pH, temperature, concentration of a protein, and the presence of a ligand are known to affect the rate of hydrogen–deuterium exchange reaction at the N_1H site of tryptophan side chains (Cassels et al., 1978; Wedin et al., 1982). In the case of lysozyme, the order of exchange rate for Trp-108 and -123 reverses with pH. This is a result of self-association of lysozyme (Sophianopoulos & Van Holde, 1964), which occurs at a pH above 5 and reduces the exchange rate for Trp-108 (Endo et al., 1987). Further, the hydrogen–deuterium exchange of Trp-63 and -108 becomes slow in the presence of inhibitors (Cassels et al., 1978).

In order to elucidate the relationships between lysozyme–inhibitor binding and the microenvironments of six tryptophan side chains, stepwise deuteriation at tryptophan N_1's was made by two different methods. In the first method, a desired number of tryptophan side chains were predeuteriated in D_2O solution without an inhibitor, and then the inhibitor [GlcNAc or $(GlcNAc)_3$] was added to the deuteriated lysozymes. The best conditions for the stepwise deuteriation were determined by use of the 1382-cm^{-1} Raman band [W6(ND)], whose intensity is an indicator of the number of N_1-deuteriated tryptophans (Takesada et al., 1976; Miura et al., 1988). The N_1-deuteriated tryptophan side chains were identified by ^1H NMR spectroscopy. Three of six tryptophans were selectively deuteriated 30 min after dissolution at 23 °C (3D3H). The percentages of deuteriated molecules were estimated from the NMR spectrum to be 100% for Trp-62 and -63, 85% for Trp-123, 15% for Trp-108, 5% for Trp-111, and 0% for Trp-28.[2] Additionally, Trp-108 was deuteriated in 6 h at 23 °C (the degree of deuteriation: 100% for Trp-62, -63, and -123, 90% for Trp-108, 15% for Trp-111, and 0% for Trp-28; 4D2H), and every tryptophan except Trp-28 was completely deuteriated in 20 min at 50 °C (5D1H). This method was adopted to investigate the microenvironments of Trp-108, -111, and -28.

In the second method, tryptophan side chains were deuteriated for lysozyme in the presence of GlcNAc. Commercially available α-GlcNAc was preequilibrated (mixture of α- and β-GlcNAc, to be termed GlcNAc) by dissolving it in H_2O at room temperature for one day to avoid mutarotation during deuteriation of tryptophan side chains in the complex. The time course of the intensity increase of the 1382-cm^{-1} band showed that only one tryptophan side chain was deuteriated 30 min after dissolution in GlcNAc–D_2O at 3 °C, another tryptophan was deuteriated 7 h at 10 °C, and the third was deuteriated 2 h at 28 °C. The order of exchange rates, determined by use of ^1H NMR spectra, was Trp-62 > 123 > 63, which is consistent with a previous result at pH 4.0 (Cassels et al., 1978). Separate deuteriation of Trp-62 and -63 became possible in the presence of GlcNAc because the inhibitor binding reduced the exchange rate of Trp-63 considerably. $(GlcNAc)_3$ could not be used in the stepwise deuteriation

[2] The order of exchange of Trp-108 and 123 was reversed in our previous paper (Miura et al., 1988), since the exchange rates reported for pH 3.8 solutions (Wedin et al., 1982) were assumed.

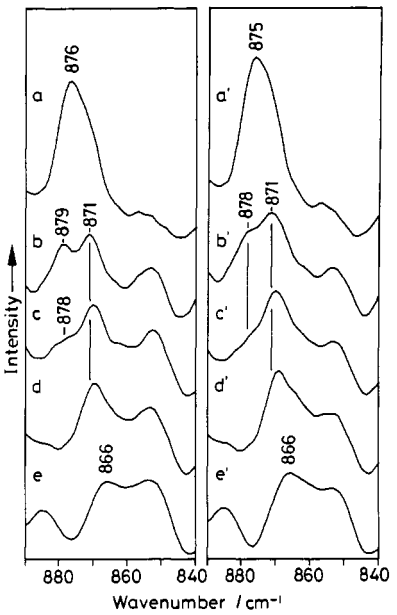

FIGURE 1: Raman spectra (890–840 cm^{-1}) of lysozyme (left) and lysozyme–$(GlcNAc)_3$ (right) in H_2O (a) and stepwise-deuteriated lysozyme in D_2O: (b) 3D3H, (c) 4D2H, (d) 5D1H, (e) 6D. The intensity is normalized to that of the 1004-cm^{-1} band of phenylalanine.

because of marked broadening of resonance lines in the ^1H NMR spectra (Blake et al., 1981) that made assignments of deuteriated tryptophan side chains impossible.

RESULTS

Inhibitor Binding and the States of H-Bonding of Tryptophan Side Chains

(A) Trp-28, -108, and -111. The Raman spectrum (890–840-cm^{-1} region) of lysozyme in H_2O solution is shown in Figure 1a. A band at 876 cm^{-1} is assigned to the tryptophan W17 mode (Harada & Takeuchi, 1986), and a weak band around 855 cm^{-1} is the high-frequency component of the tyrosine doublet (Siamwiza et al., 1975). W17 is a mixed mode of the benzene-12-like vibration and N_1H motion, and hence it shifts down by about 20 cm^{-1} on N_1 deuteriation (Takeuchi & Harada, 1986). The frequency is sensitive to the strength of H-bonding at the N_1 site: it is 883 cm^{-1} for non-H-bonding tryptophan derivatives and becomes lower toward 871 cm^{-1} as the H-bonding strength increases (Miura et al., 1988). The broad and unsymmetrical band shape of W17 in Figure 1a arises from an overlap of those of six side chains with different H-bonding states. However, it was possible to identify the peaks of individual side chains by utilizing the above-mentioned characteristics of W17 and difference spectra of stepwise N_1H deuteriated lysozyme: 879 (Trp-108), 878 (Trp-111), 877 (Trp-62 and -63), 875 (Trp-123), and 871 cm^{-1} (Trp-28) (Miura et al., 1988).

Figure 1b shows the spectrum of a D_2O solution of lysozyme in which three tryptophan side chains, Trp-62, -63, and -123, are selectively deuteriated (3D3H). The W17 band consists of two peaks at 879 (due to Trp-108 and -111) and 871 cm^{-1} (Trp-28). The three deuteriated tryptophans give a W17(ND) band around 860 cm^{-1} overlapping with the tyrosine band whose frequency and intensity may also change on deuteriation of the phenolic hydroxyl group. The intensity of the 879-cm^{-1} peak decreases on deuteriation of the fourth tryptophan, Trp-108 (4D2H; Figure 1c), and disappears when the fifth, Trp-111, is deuteriated (5D1H; Figure 1d). The low-frequency component at 871 cm^{-1} disappears on deuteriation of the last tryptophan, Trp-28 (6D; Figure 1e). A double-peaked broad

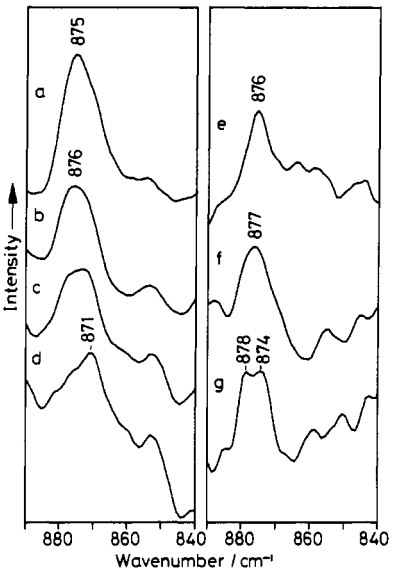

FIGURE 2: Raman spectra (890–840 cm^{-1}) of an aqueous solution of lysozyme–GlcNAc in H_2O (a, 6H), stepwise-deuteriated lysozyme–GlcNAc in D_2O (b–d), and difference spectra (e–g): (b) 1D5H, (c) 2D4H, (d) 3D3H, (e) 6H – 1D5H, (f) 1D5H – 2D4H, and (g) 2D4H – 3D3H. The intensity scale is the same as in Figure 1.

feature in the 870–850-cm^{-1} in Figure 1e is due to an overlap of W17(ND)'s of six tryptophans and the high-frequency component of tyrosine doublet of three (possibly deuteriated) tyrosines.

Raman spectra of these lysozymes mixed with $(GlcNAc)_3$ are shown on the right side of Figure 1. [$(GlcNAc)_3$ does not give any strong Raman bands in this region at the concentration adopted here.] The W17 frequencies in the difference spectra, 3D3H – 4D2H, 4D2H – 5D1H, and 5D1H – 6D (not shown), are identical with those of the free lysozymes. Trp-28, -108, and -111 are located in the hydrophobic box, and some H-bonds are formed within or near the region, e.g., N_1H of Trp-28 is H-bonded to the main-chain carbonyl group of Tyr-23 in the hydrophobic box and that of Trp-111 to the side chain of Asn-27, which lies next to the box (Diamond et al., 1971). The invariance of the W17 frequencies indicates that the network of H-bonding is maintained against the inhibitor binding. On the other hand, the W17 intensities of lysozyme–$(GlcNAc)_3$ differ from those of free lysozyme. In particular, the 871-cm^{-1} band due to Trp-28 is strong in the complex. The reason will be discussed later. A similar investigation was conducted by using GlcNAc (spectra not shown), and the same peak frequencies for the three tryptophan side chains and the intensity increase of the 871-cm^{-1} band were observed.

(B) Trp-62, -63, and -123. The W17 frequencies of these three tryptophan side chains in the inhibitor-bound state were investigated by using precomplexed lysozyme–GlcNAc. The Raman spectra of complexed lysozymes (6H, 1D5H, 2D4H, and 3D3H; see Experimental Procedures) and the differences are shown in Figure 2.

Lysozyme–GlcNAc is regarded as an approximately equimolar mixture of lysozyme–α-GlcNAc and lysozyme–β-GlcNAc (Blake et al., 1967; Dahlquist & Raftery, 1968). According to an X-ray crystallographic study on lysozyme–GlcNAc (Blake et al., 1967), β-GlcNAc is so positioned as to make H-bonds between its O_6 and O_3 atoms and the indole N_1H's of Trp-62 and -63, respectively, in subsite C. This binding form is essentially identical with that observed for lysozyme–$(GlcNAc)_3$ (Blake et al., 1967). α-GlcNAc also binds to subsite C but in a different way, in which no H-bond

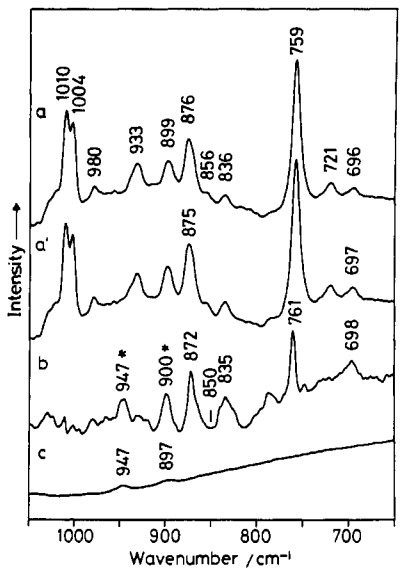

FIGURE 3: Raman spectra of free lysozyme (a), lysozyme–$(GlcNAc)_3$ (a'), and $(GlcNAc)_3$ (c) in H_2O solution, and the a' – a spectrum (b). The Raman intensity in spectra a and a' is normalized to that of the 1004-cm^{-1} band of phenylalanine, but the intensity of the difference spectrum b is magnified by five. The bands marked with an asterisk in spectrum b are contributed by $(GlcNAc)_3$.

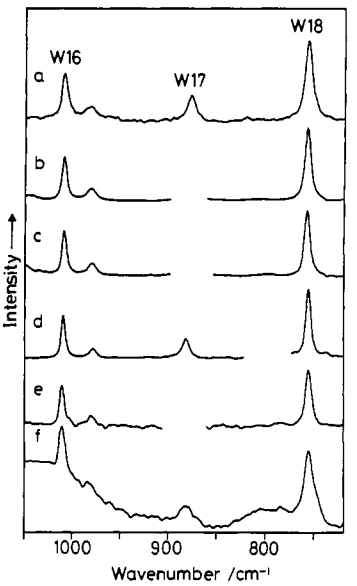

FIGURE 4: Raman spectra of skatole solution (a–e; 50 mM) and vapor (f; about 500 Torr at 140 °C). The solvents are (a) H_2O (90 °C), (b) H_2O–ethanol (50% v/v), (c) ethanol, (d) carbon disulfide, and (e) cyclopentane. Raman scattering of the solvents has been subtracted, but the regions where strong solvent bands overlap are left blank.

from Trp-62 or -63 is formed. Two W17 peaks at 878 and 874 cm^{-1} due to Trp-63 (Figure 2g) suggest that the H-bond formation between Trp-63 and GlcNAc observed in the crystalline state is conserved in the solution. The low-frequency peak indicates that the H-bond between Trp-63 and β-GlcNAc is strong, because it is located between 877 (a moderate H-bond with solvent water) and 871 cm^{-1} (a very strong H-bond; Miura et al., 1988). The W17 frequency of Trp-62, 876 cm^{-1} (Figure 2e), in the complex, indicates that the N_1H group of Trp-62 takes part in an H-bond which is as weak as that with the solvent.

Although Trp-123 is located at the molecular surface far from the active site (Blake et al., 1967), the W17 due to this side chain exhibits an upward shift from 875 (Miura et al., 1988) to 877 cm^{-1} (Figure 2f) upon GlcNAc binding. This result indicates a structural change around the N_1H site of Trp-123.

Intensity Changes Caused by Inhibitor Binding

Raman spectra of lysozyme and lysozyme–$(GlcNAc)_3$ in H_2O solution are shown in Figure 3, a and a', respectively. Intensities are normalized to that of the 1004-cm^{-1} band of phenylalanine. This band was unaffected by the inhibitor binding as was a band at 1447 cm^{-1} (due to the CH bending vibrations of aliphatic side chains) which is often used as an internal intensity standard of Raman spectra of proteins. The intensities at 1010 cm^{-1} due to tryptophan (W16), 933 cm^{-1} due to the main chain, and 721 cm^{-1} due to cystine also do not show detectable changes. On the other hand, a significant intensity change is observed in two tryptophan bands at 759 (W18) and 876 cm^{-1} (W17), a tyrosine doublet at 856/836 cm^{-1}, and a methionine band at 696 cm^{-1} (Figure 3b). Details on individual groups are described below.

Tryptophan Side Chains. The strong band around 760 cm^{-1} in Figure 3 is assigned to the indole ring breathing vibration, W18 (Harada & Takeuchi, 1986; Takeuchi & Harada, 1986). It exhibits significant intensity increase upon the inhibitor binding. In order to know the factors affecting the W18 intensity, we studied Raman spectra of skatole in several solvents and in the vapor as models of tryptophan side chains in proteins (Figure 4). The W18 intensity is evaluated against the W16 band whose intensity is not affected by the inhibitor binding (Figure 3). The integrated intensity is strongest for H_2O solution and becomes weaker for H_2O–ethanol, ethanol, carbon disulfide, and cyclopentane in that order. On the other hand, the intensity of skatole in the vapor phase (Figure 4f and Table I) is about the same as or even stronger than that in H_2O. Hence, a tryptophan side chain without hydrophobic interactions with neighboring groups is expected to give a strong W18 band whether it is buried in the interior or not.

Table I: Frequencies (cm^{-1}) and Intensities[a] of W17 and W18 Bands of Skatole

	W17		W18	
	ν	intensity	ν	intensity
H_2O	878	0.76 (0.55)	758	2.40 (1.88)
H_2O–ethanol (50%)			758	2.28 (1.76)
ethanol			758	2.10 (1.62)
carbon disulfide	883	0.75 (0.50)	757	1.67 (1.52)
cyclopentane			757	1.63 (1.35)
vapor	883	0.63 (0.38)	757	2.61 (1.66)

[a] Integrated intensity (peak intensity) relative to that of the W16 band at 1010 cm^{-1}.

In lysozyme the W18 band is an overlap of those due to six tryptophan side chains. On the left of Figure 5 are shown the Raman spectra in the W18 region of stepwise-deuteriated lysozymes. The peak frequency shifts down gradually as the deuteriation proceeds, indicating that each W18 component shows a downward frequency shift upon deuteriation (Takeuchi & Harada, 1986). A similar trend is observed also for the lysozyme–$(GlcNAc)_3$ complex (Figure 5, center). The difference spectrum between lysozyme–$(GlcNAc)_3$ and free lysozyme at each step of deuteriation shows an increase in intensity upon inhibitor binding (Figure 5, right). Since the peak frequency in the difference spectra changes between 4D2H and 5D1H concomitant with deuteriation of the fifth tryptophan (Trp-111), the significant increase in intensity upon the complex formation must arise from a decrease in hydrophobic interaction between Trp-111 and the neighboring aliphatic groups.

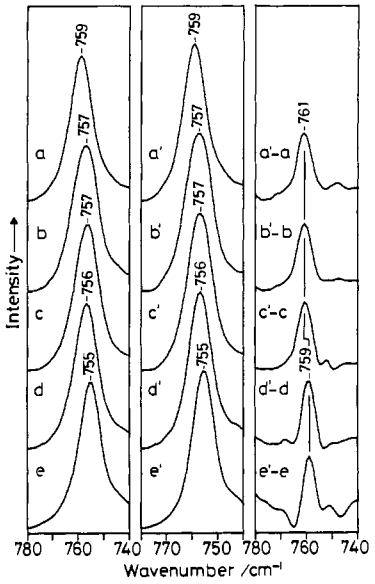

FIGURE 5: Raman spectra (780–740 cm^{-1}) of stepwise-deuteriated lysozyme (left), lysozyme–$(GlcNAc)_3$ (center), and difference spectra (right) between lysozyme–$(GlcNAc)_3$ and free lysozyme (center, left). (a) 6H, (b) 3D3H, (c) 4D2H, (d) 5D1H, and (e) 6D.

A strong positive W17 peak at 872 cm^{-1} in the difference spectrum (Figure 3b) is ascribed to the intensity increase of a strongly H-bonded tryptophan, Trp-28. Raman spectra of stepwise-deuteriated lysozyme confirm this assignment, because the 871-cm^{-1} band due to Trp-28 of lysozyme–$(GlcNAc)_3$ is stronger than that of free lysozyme at the corresponding steps of deuteriation (Figure 1).

The W17 intensity of the Bence-Jones protein is much stronger than that of the amino acid tryptophan and becomes weak on denaturation (Kitagawa et al., 1979). Such a high intensity has been ascribed to tryptophan side chains buried in the interior of the protein (Kitagawa et al., 1979). A description such as "buried", however, cannot explain the significant intensity increase of W17 observed here, because Trp-28 is completely buried in the protein interior whether the inhibitor is bound or not (Glickson et al., 1971; Imoto et al., 1972; Cassels et al., 1978). The intensity increase may be caused by a change in environment of buried Trp-28. The W17 band of skatole has comparable intensities in carbon disulfide and H_2O solutions, which are slightly greater than that in the vapor (Figure 4 and Table I). Thus, interactions stronger than the solute–solvent ones must be responsible for the distinct intensity increase of the W17 band of Trp-28.

In the Raman spectra of L-tryptophan and its derivatives in solution, the W17 intensity is about one-third that of W16 [e.g., the relative intensity, I(W17)/I(W16) is 0.32 for L-tryptophan in H_2O solution; Harada et al., 1986)]. However, it is quite strong in crystals of some tryptophan derivatives (Miura et al., 1989): crystalline powders of Ac-L-TrpME and Ac-DL-TrpMA give 0.92 and 0.89, respectively. According to an X-ray study (Cotrait & Barrans, 1974), the indole ring of Ac-L-TrpME is in close contact with ester methoxy groups of adjacent molecules from both sides of the ring plane (perpendicular distances from the carbon atoms in the methoxy groups to the indole ring plane are 3.4 and 3.7 Å, respectively). Such short distances suggest the presence of very strong van der Waals interactions. A similar situation is seen in the crystal structure of Ac-DL-TrpMA (Harada & Iitaka, 1977). On the other hand, crystalline L-Trp-HCl gives a normal W17 intensity [I(W17)/I(W16), 0.36], and the crystal structure does not show any strong interaction involving the indole ring (Takigawa et al., 1966). These results lead to the conclusion that a very close van der Waals contact between the indole ring of tryptophan and aliphatic groups, which is realized only in special cases such as protein interior or crystals, induces a distinct intensity increase of the W17 band.

Tyrosine Side Chains. The intensity ratio of tyrosine doublet at 850/830 cm^{-1} is known to be sensitive to the states of H-bonding at the phenolic OH group (Siamwiza et al., 1975). The ratio of the 856/836-cm^{-1} doublet is 0.47 in free lysozyme and decreases to 0.28 upon binding to $(GlcNAc)_3$ (Figure 3), which suggests a change in the H-bonding states of tyrosine side chains. Hen lysozyme has three tyrosine residues at sequence positions 20, 23, and 53, and they are located around the active site (Blake et al., 1967). Among them Try-53 is the only tyrosine that takes part in intramolecular H-bonding in crystal (to Thr-51 and from Asp-66; Imoto et al., 1972), and Tyr-20 and -23 are not H-bonded to particular groups. Upon binding to the inhibitor, the latter two do not seem to form H-bonding with the inhibitor (Blake et al., 1967). Presumably, the observed charge in the intensity ratio is caused by change in H-bonding of Tyr-53.

Methionine Side Chains. Two bands at 721 and 696 cm^{-1} in Figure 3a arise from the CS stretch modes. The 696-cm^{-1} band has been assigned to methionine (Lord & Yu, 1970). Since hen lysozyme has two methionine residues, 12 and 105, both in the TG form about the axes in $C_\alpha C_\beta$–C_γ–$S_\delta C_\epsilon$ (Diamond et al., 1971), the band is assigned to an overlap of the CS stretch bands of the two methionines in the TG form, which is supported by the frequency-conformation correlations proposed on the basis of vibrational analysis on model compounds (Nogami et al., 1975). The 721-cm^{-1} band may be assigned to an overlap of several CS stretching bands in the P_C and P_N forms (trans CC_α–$C_\beta S$ and trans NC_α–$C_\beta S$ forms, respectively) of eight half-cystines. It is known that the CS stretch band around 665 cm^{-1} of the P_H form (trans HC_α–$C_\beta S$ form) is much stronger than those of the P_C and P_N forms (Bastian & Martin, 1973). However, since most of the conformations in lysozyme are P_C and P_N ($5P_C$, $2P_N$, and $1P_H$; Harada & Takeuchi, 1986), the 721-cm^{-1} band must appear clearly. The inhibitor binding seems to induce an intensity increase of the methionine CS stretch band in contrast to the invariance of the cystine band, which suggests an environmental change around Met-12 or/and -105. However, it is also possible that the 696-cm^{-1} band is contributed from tryptophan side chains and the observed intensity increase is partly due to an environmental change of the tryptophan side chains, because tryptophan and its derivatives give a weak band in the 710–697-cm^{-1} region (Miura et al., unpublished data).

DISCUSSION

Rearrangement of Side Chains in the Hydrophobic Box upon Inhibitor Binding. The experimental results on the environmental changes of Trp-28 and -111 upon $(GlcNAc)_3$ binding are summarized below. (1) The states of H-bonding at N_1H for both tryptophan indoles are not affected by the inhibitor binding because their W17 frequencies are unchanged. (2) The hydrophobic interaction of the indole ring of Trp-111 becomes weaker in the complex on the basis of the increased W18 intensity of Trp-111. (3) The indole ring of Trp-28 interacts with neighboring aliphatic side chains more strongly in the complex as indicated by the increased W17 intensity of Trp-28.

The second and third observations indicate that the inhibitor binding induces structural changes in the hydrophobic box, in accord with the shifts of NMR peaks of Trp-28 and -111 upon inhibitor binding (Perkins & Dwek, 1980; Blake et al.,

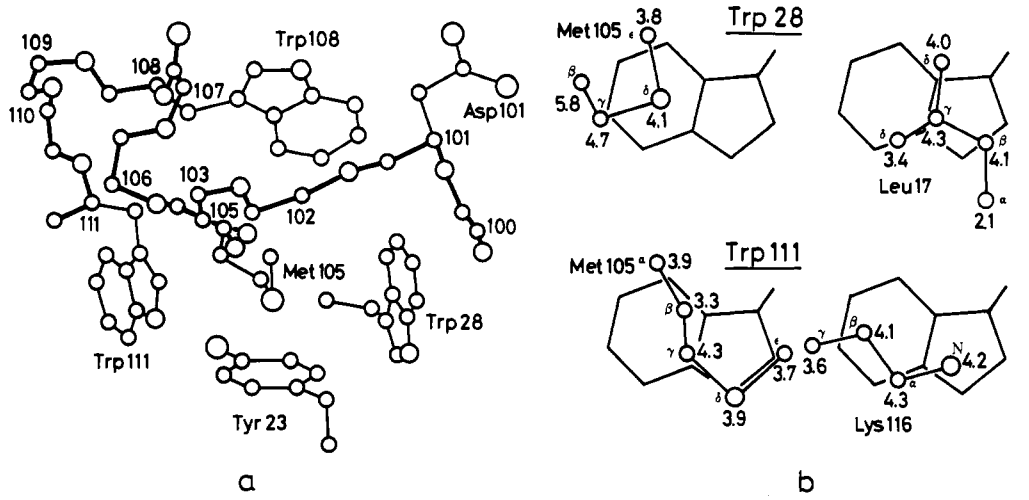

FIGURE 6: (a) Structure in the hydrophobic box region of hen lysozyme (Diamond et al., 1974); the main chain 100–111 and the side chains of Tyr-23, Trp-28, Asp-101, Met-105, Trp-108, and Trp-111 are shown. (b) Microenvironments of the Trp-28 and -111 side chains. The left- and right-hand sides of the figure show neighboring atoms inside and outside the hydrophobic box, respectively. The numerical value given for each atom indicates the distance (Å) from the plane of indole ring.

1981; Bernard et al., 1990). On the other hand, the first observation suggests that the structure in the vicinity of N_1H parts of the two indole rings remains practically unchanged. These findings are interpreted consistently by supposing a movement of the Met-105 side chain, which is located between the indole rings of Trp-28 and -111 (Figure 6a), toward Trp-28. The terminal methylsulfide group of Met-105 in the free enzyme is in close contact with the two indole rings at almost equal distances (Figure 6b). Accordingly, even a small shift of Met-105 away from Trp-111 toward Trp-28 may cause a large decrease in the van der Waals interaction between Met-105 and Trp-111 and a concomitant increase between Met-105 and Trp-28. The changes in the hydrophobic interaction of Trp-28 and -111 have been detected in the intensity of W17 band. As stated above, the W17 band of Trp-28 at 871 cm^{-1} increases in intensity upon inhibitor binding, reflecting the increased hydrophobic interaction. An indication of concomitant environmental change around Trp-111 is seen in the Raman spectrum of lysozyme–$(GlcNAc)_3$ in the 4D2H state (Figure 1c′). A shoulder peak at 878 cm^{-1} due to Trp-111 is much weaker than that in free lysozyme (Figure 1c), which is ascribed to a decrease in the hydrophobic interaction. Therefore, the environmental changes monitored by the W17 intensity is consistent with the movement of Met-105 from Trp-111 to Trp-28.

It has been shown that the W18 intensity of Trp-111 increases on inhibitor binding and this observation is again consistent with weakened van der Waals interaction with Met-105. However, concomitant intensity decrease expected for Trp-28 is not detected in the Raman spectra. This is probably because the W18 bands of six tryptophan side chains are unresolvable and the decrease in intensity of Trp-28 is covered by much larger increase of Trp-111. In a crystal, Trp-28 is in close contact with a terminal methyl group of Leu-17 outside of the hydrophobic box, while the nearest outside neighbor of Trp-111, Lys-116, is located more than 4 Å apart from the indole ring (Figure 6b). Hence, the shift of the Met-105 position toward Trp-28 would cause a change in hydrophobicity around Trp-111 much greater than that around Trp-28. The Raman intensity changes of Trp-28 and -111 are consistent with the rearrangement of the sandwich structure composed of Trp-28, Met-105, and Trp-111.

Role of the Hydrophobic Box in Inhibitor Binding. Although the side chains of Trp-28, -111, and Met-105 lie near the active site, they are not directly in contact with an incorporated inhibitor molecule (Blake et al., 1967). However, these residues are conserved in many chicken-type lysozymes (Jollès & Jollès, 1984). Met-105 belongs to loop 100–107, which connects two α-helices 91–99 and 108–114 and is expected to be rather flexible owing to two glycines at positions 102 and 104. Most of the loop is exposed to the active site cleft, and some residues of the loop interact with the inhibitor molecule (Blake et al., 1967); e.g., the side chain of Asp-101 and the main-chain carbonyl of Ala-107 form H-bonds with an incorporated $(GlcNAc)_3$. In particular, the H-bond involving Ala-107 may well influence the conformation of loop 100–107, because the most significant change upon inhibitor binding has been detected around Ala-107 by an X-ray crystallographic study on lysozyme–inhibitor complexes (Bernard et al., 1990). In contrast to the general flexibility of the loop, a small portion at 104–106 is tightly bent, and the side chain of Met-105 is wedged in between two indole rings of Trp-28 and -111 (Figure 6a) belonging to α-helices 25–35 and 108–114, respectively (Blake et al., 1965). Thus the hydrophobic box is regarded as a contact region of the rigid hydrophobic core and the flexible loop at the active site. The high hydrophobicity around Trp-28 in lysozyme–$(GlcNAc)_3$ indicates that the strain caused by the inhibitor binding on the active site is transferred to Trp-28 through the movement of Met-105. It is tempting to speculate that the hydrophobic box assists the enzymatic function by preventing disruption of the appropriate conformation for the activity. This may be an example of a well-designed molecular architecture for enzymatic functions.

Conclusion

The states of six tryptophan side chains in hen lysozyme bound to substrate-analogous inhibitors were investigated by a combination of hydrogen → deuterium exchange labeling and Raman difference spectroscopy. The W17 frequencies of individual side chains were useful in elucidating the states of H-bonding in the complexes. The H-bond strength at the N_1 sites of Trp-62 in the active site and of Trp-28, -108, and -111 in the protein interior remained unchanged upon inhibitor binding. On the other hand, the doublet W17 peaks at 878 and 874 cm^{-1} arising from Trp-63 strongly suggested the presence of lysozyme–α-GlcNAc and lysozyme–β-GlcNAc, respectively, and a specific H-bonding between Trp-63 and

β-GlcNAc in the latter complex. This specific and strong H-bonding implies an important contribution of Trp-63 to the substrate binding.

Inhibitor binding induced increases in the W17 intensity of Trp-28 and the W18 intensity of Trp-111. Such changes have been explained as a result of a shift in position of Met-105 away from Trp-111 toward Trp-28 in the hydrophobic box. A possible role of the sandwich arrangement of Trp-111·Met-105·Trp-28 in the enzymatic activity has been suggested.

Registry No. Trp, 73-22-3; Met, 63-68-3; skatole, 83-34-1.

References

Bastian, E. J., Jr., & Martin, R. B. (1973) *J. Phys. Chem. 77*, 1129–1133.

Berger, L. R., & Weiser, R. S. (1957) *Biochim. Biophys. Acta 26*, 517–521.

Bernard, M., Canioni, P., Cozzone, P., Berthou, J., & Jolles, P. (1990) *Int. J. Pept. Protein Res. 36*, 46–55.

Blake, C. C. F., Koenig, D. F., Mair, G. A., North, A. C. T., Phillips, D. C., & Sarma, V. R. (1965) *Nature (London) 206*, 757–761.

Blake, C. C. F., Johnson, L. N., Mair, G. A., North, A. C. T., Phillips, D. C., & Sarma, V. R. (1967) *Proc. R. Soc. London B167*, 378–388.

Blake, C. C. F., Cassels, R., Dobson, C. M., Poulsen, F. M., Williams, R. J. P., & Wilson, K. S. (1981) *J. Mol. Biol. 147*, 73–95.

Cassels, R., Dobson, C. M., Poulsen, F. M., & Williams, R. J. P. (1978) *Eur. J. Biochem. 92*, 81–97.

Cotrait, P. M., & Barrans, Y. (1974) *Acta Crystallogr. B30*, 510–513.

Dahlquist, F. W., & Raftery, M. A. (1968) *Biochemistry 7*, 3269–3277.

Diamond, R., Phillips, D. C., Blake, C. C. F., & North, A. C. T. (1971) Brookhaven Protein Data Bank, 2LYZ.

Endo, T., Ueda, T., Yamada, H., & Imoto, T. (1987) *Biochemistry 26*, 1838–1845.

Glickson, J. D., Phillips, D. C., & Rupley, J. A. (1971) *J. Am. Chem. Soc. 93*, 4031–4038.

Harada, Y., & Iitaka, Y. (1977) *Acta Crystallogr. B33*, 244–247.

Harada, I., & Takeuchi, H. (1986) in *Spectroscopy of Biological Systems, Advances in Spectroscopy* (Clark, R. J. H., & Hester, R. E., Eds.) Vol. 13, pp 113–175, Wiley, Chichester.

Harada, I., Miura, T., & Takeuchi, H. (1986) *Spectrochim. Acta 42A*, 307–312.

Imoto, T., Johnson, L. N., North, A. C. T., Phillips, D. C., & Rupley, J. A. (1972) in *The Enzymes* (Boyer P. D., Ed.) Vol. 7, pp 665–867, Academic Press, London.

Jeanloz, R. W., Sharon, N., & Flowers, H. M. (1963) *Biochim. Biophys. Res. Commun. 13*, 20–25.

Jollès, P., & Jollès, J. (1984) *Mol. Cell. Biochem. 63*, 165–189.

Kitagawa, T., Azuma, T., & Hamaguchi, K. (1979) *Biopolymers 18*, 451–465.

Lord, R. C., & Yu, N. T. (1970) *J. Mol. Biol. 50*, 509–524.

Miura, T., Takeuchi, H., & Harada, I. (1988) *Biochemistry 27*, 88–94.

Miura, T., Takeuchi, H., & Harada, I. (1989) *J. Raman Spectrosc. 20*, 667–671.

Nogami, N., Sugeta, H., & Miyazawa, T. (1975) *Chem. Lett.*, 147–150.

Perkins, S. J., & Dwek, R. A. (1980) *Biochemistry 19*, 245–258.

Redfield, C., & Dobson, C. M. (1988) *Biochemistry 27*, 122–136.

Rupley, J. A. (1964) *Biochim. Biophys. Acta 83*, 245–255.

Siamwiza, M. N., Lord, R. C., Chen, M. C., Takamatsu, T., Harada, I., Matsuura, H., & Shimanouchi, T. (1975) *Biochemistry 14*, 4870–4876.

Sophianopoulos, A. J., & Van Holde, K. E. (1964) *J. Biol. Chem. 239*, 2516–2524.

Sugeta, H., Go, A., & Miyazawa, T. (1972) *Chem. Lett.*, 83–86.

Takesada, H., Nakanishi, M., Hirakawa, A. Y., & Tsuboi, M. (1976) *Biopolymers 15*, 1929–1938.

Takeuchi, H., & Harada, I. (1986) *Spectrochim. Acta 42A*, 1969–1978.

Takigawa, T., Ashida, T., Sasada, Y., & Kakudo, M. (1966) *Bull. Chem. Soc. Jpn. 39*, 2369–2378.

Wedin, R. E., Delepierre, M., Dobson, C. M., & Poulsen, F. M. (1982) *Biochemistry 21*, 1098–1103.